Hindawi
Advances in Materials Science and Engineering
Volume 2022, Article ID 4805867, 10 pages
https://doi.org/10.1155/2022/4805867

Research Article

The Properties of the Tide Current and Sediment at a Port of Southern China

Hongyan Shen,[1,2] **Ruicai Xie**,[3] **and Liqin Song**[1,2]

[1]*Key Laboratory of Ministry of Education for Coastal Disaster and Protection, Hohai University, Nanjing 210024, China*
[2]*College of Harbor, Coastal and Offshore Engineering, Hohai University, Nanjing 210024, China*
[3]*CCCC-FHDI Engineering Co., Ltd, Haizhu District, Guangzhou 510230, China*

Correspondence should be addressed to Hongyan Shen; shenhongyan78@hhu.edu.cn

Received 29 December 2021; Accepted 31 January 2022; Published 4 March 2022

Academic Editor: Yonghong Wang

Environmental factors of projects in the sea area, such as tidal current characteristics and sediment transport patterns, play a decisive role in the safe operation of the harbor. Based on the observation data of tide level, tidal current, suspended sediment, and surface sediment in the Port of Shenquan, this paper focuses on the study of the characteristics of tidal current and sediment of projects in the sea area. According to the measured tide hydrograph, it can be concluded that the tide in the Port of Shenquan is irregular diurnal, and the flow of rising and falling tides is basically rectilinear. The velocity of the neap tide is higher than that of spring tide, which is mainly related to the strong winds and waves. The sand source is limited, and the sediment concentration in the water is very low. The hourly sediment concentration in each station fluctuates within a narrow range, independent of hourly velocity change. The sediment is coarse and fine, with a distribution pattern of coarse near shore, fine in deep water, coarse in East and West, and fine in the middle, and the sorting coefficient of sediment is medium to well.

1. Introduction

The Coastal zone is a complex dynamic system, which is constantly affected by the change of sea level, sediment deposition, and erosion [1, 2]. The morphological evolution characteristics of estuaries are generally recognized as hydrodynamic responses from riverbanks and riverbed [3–5]. The mechanism of dynamic response depends on the environmental factors such as wave, tide, and sediment deposition in the particular estuary [6]. Due to its significant influence in the process of implementing development plan and promoting the globalization of industrial transportation of national and regional economies, the harbor is considered the "golden zone" of the socioeconomic development of the marine sectors.

The project of this paper is located in the coastal area of Huilai County, Jieyang City, Guangdong Province, China (See Figure 1). It sits in the tangent section of the sandy arc coast of Port of Shenquan, with a land area of 1253 m^2. It is adjacent to Shantou City in the East, Lufeng City in the west, Nanhai City in the South, and Puning City in the north. The Port of Shenquan is a significant place for China's economic development and layout along the Longjiang River, an important node of modern logistics, and an essential hub of core ports and regional comprehensive transportation system in the coastal areas of Guangdong Province [7, 8]. Construction in the harbor has changed nature and caused a strong disturbance to the coastal system, resulting in a new imbalance [9, 10]. They even triggered geological disasters of instability of the coastal slope [11–13], causing great damage to the infrastructure. It is useful to prevent the occurrence of slope instability if the interaction mechanism of the hydrodynamic environment of the harbor and the slope is thoroughly considered.

The port is usually with a large amount of sediment and ascribing to some external hydrodynamic forces such as tides and currents. The sediment will undergo complex movements, namely, sedimentation and suspension, which leads to channel sedimentation, estuarial and coastal changes, water pollution, and other ecological problems

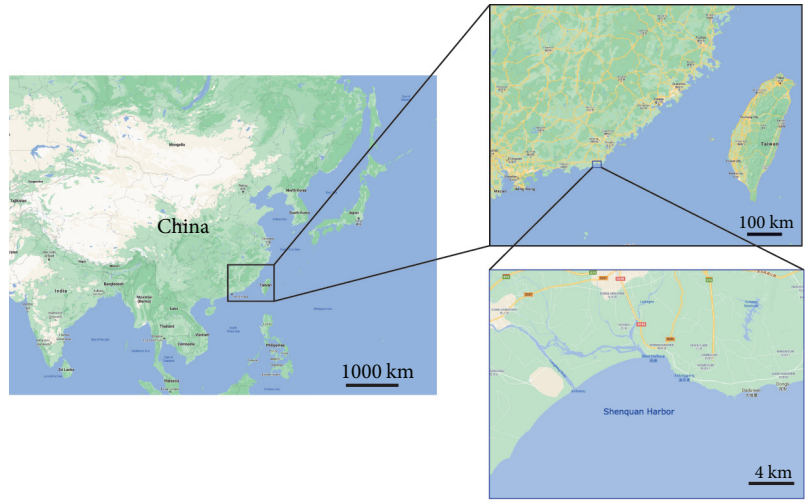

Figure 1: The spatial location of the port of Shenquan and the research area.

[14–18]. These problems must be considered and solved in hydraulic engineering [19], coastal engineering, port, and waterway engineering in coastal and estuarial areas. Due to incoming tides and waves, sediment is generally formed in tidal estuary and wave dominated estuary on the landward side [20–22]. The flow direction and sediment entrainment in the coastal zone are mainly driven by the simultaneous action of swell and tide [23]. Sediment transport is mainly composed of bed sediment and suspended sediment [24–26]. Channel siltation caused by tidal sediment movement is one of the main problems in ports. However, the deposition rate of sediments varies among different ports, which depends on the wave and the characteristics of rock and soil [27–29]. Maintenance dredging is of great necessity if channel siltation reduces the available depth for safe navigation of ships. In determining the location and design of the layout of the port, it is crucial to consider the characteristics of the environment and the riverbed/suspended sediment.

Tidal current is one of the main hydrodynamic factors of a port, which exerts great influences on the diffusion and drift of pollutants in coastal waters, the design of the infrastructure of the port, and navigation safety [30]. Construction of a port changes the contour of the coastline, breaks the original dynamic balance between hydrodynamic force and seabed, and causes the redistribution of tidal capacity, resulting in the changes of hydrodynamic force and sediment deposition in the estuary and coast [31–33]. Many scholars have carried out a lot of research on the characteristics of sediment particle size, sediment transport, and sedimentary environment evolution in port and coastal areas, to explore environmental information such as regional estuarine and coastal sedimentary dynamics, sediment sources, and sediment transport trends by analyzing the grain size characteristics of sediments [34–37]. Therefore, by analyzing the tidal current and sediment properties of the engineering sea area, the study of the hydrodynamic process of the port under the action of tide is of great practical significance for the normal operation of the port, public safety, and marine environment management.

This paper is to study the characteristics of the tide current and sediment based on the field observations at the Port of Shenquan. Ii is divided into four parts: Section 1 is an introduction; Section 2 mainly introduces the study area and data collecting methods; Section 3 involves the results and the corresponding discussions; the main conclusions and perspectives are given in Section 4.

2. Field Observation of the Tide Current and Sediment

2.1. Location of the Research Area. The arc-shaped coast of the Shenquan Bay (See Figure 2) is a sandy coast developed in the southwest of Aojiao Shenquan granite platform in the post glacial period, where the Longjiang River and Leiling river systems converge into the sea. Longjiang and Leiling river systems are developed in Mesozoic granite and quartz sandstone distribution areas where the ground weathering is intensive [38]. Since the sea level was relatively stable 6000 years ago, a large amount of sediment brought by rivers and original land slopes gradually filled the ancient Port of Shenquan under the collaborations of powers from river and ocean (tides, currents, and waves), and molded it into the present appearance with a logarithmic spiral coastal profile. Shenquan Bay is open to the south with a width of opening more than 20 km. The coastline of the upper promontory (from Aojiao to Yutoujiao) is from Northeast to Southwest, which renders poor barrier and protection. The slope of the beach is gentle, about 1/700. The surface sediment in the bay is mainly fine sand, and high-tide shoreline is covered by vegetation. The area of the study is mainly confined by the wind, wave, tide, and other marine dynamic conditions and is also affected by the topography, sediment of the Bay and the Longjiang River.

2.2. Tide Level Observation. A temporary tide station is set up at the design position for synchronous continuous tide level observation (see Figure 2), and a water gauge is set up

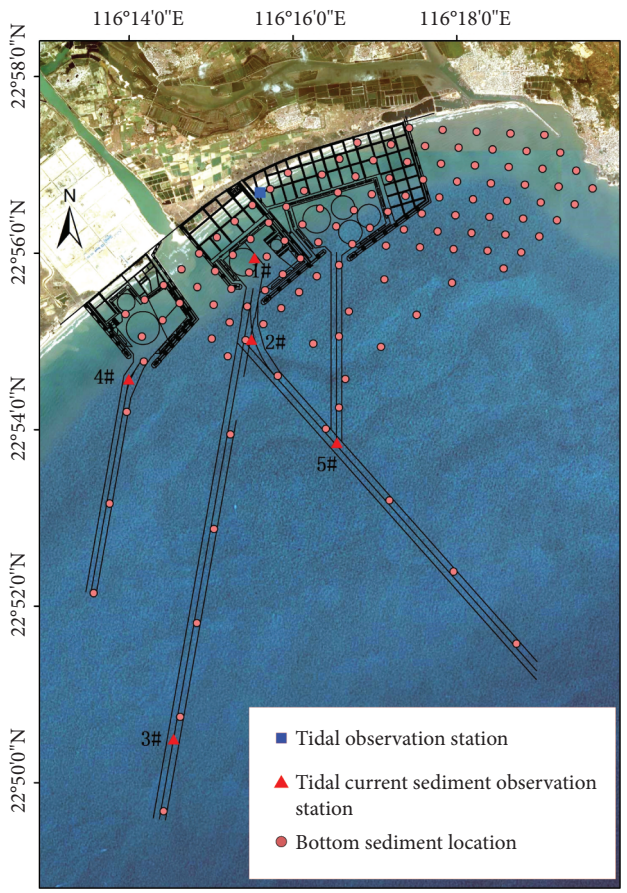

Figure 2: Observation stations and the bottom sediment data acquisition locations.

on land to check the tide level. The tide level data after land correction are calculated according to the relationship between average sea level and then the tide level correction is carried out. The national 1985 elevation datum is adopted. The AQUAlogger520 is placed near the water gauge to observe for 30 consecutive days. The observation on land is recorded every 10 minutes every half hour before and after the high tide every day and the water gauge reads to 0.01 M. A stable level and working level are set near the water gauge. The NA2 automatic level is used to measure the fourth level elevation, and the ordinary level is used for the survey from the working level to the zero elevation of the water gauge. Zero elevation shall be calibrated at the beginning and end to ensure the accuracy of the data.

2.3. Tidal Current and Sediment Observation. There are 5 measuring stations for tidal current and sediment observation (see Figure 2), among which Station 1 is located in the water area of the proposed port, Station 2\3 and 5 are located in the water area of the approach channel, and Station 4 is located in the water area near the Sinopec crude oil terminal. The test items include velocity, flow direction, and sediment concentration. The velocity and direction of flow are mainly observed by Doppler Current Profiler and compared with the traditional SLC9-2 direct reading current meter. The observation method is a synchronous six-point method. CTD temperature salt depth turbidimeter was used to observe the sediment concentration, which was synchronous with the velocity. CTD temperature salt depth turbidimeter is set to record data every 0.2 m. 1000 ml of water sample was collected simultaneously at high and low tides, rising and falling tides, and the corresponding sediment concentration was calculated by filtration, drying, and weighing, and then it was compared with the sediment concentration measured by CTD. Three tide types, large, medium, and small, were selected to observe the diurnal full tide test for more than 26 hours at each station.

2.4. Bottom Sediment Observation. According to the technical requirements of tidal current and sediment observation, 13 sections are arranged in the sea area of the project, including 10 sections in the coastal waters and 3 sections in the approach channel. 3–14 sampling points are set in each section, with a total of 122 surface sediment samples (see Figure 2). Each sediment sample shall not be less than 1 kg. GPS is used to direct the survey ship to the sampling points, and the mussel sampler is used to take samples point by point. The samples were analyzed by an NSY-3 wide range particle size analyzer and NFY-D acoustic vibration automatic screening instrument, developed by Hohai University and Nanjing Institute of Geography and Limnology, Chinese Academy of Sciences, respectively.

3. Results and Discussion

3.1. Characteristics of Monthly Tide Level. According to the statistical analysis of measured tide level data, as shown in Figure 3, the average sea level of the Port of Shenquan is 1.15 m (1985 National Elevation Benchmarks), the average high and low tide levels are 1.44 m and 0.88 m, respectively, with the average tidal range of 0.56 m. The month's tide observation is a short period from neap tide to spring tide and then to the neap tide. Therefore, the daily average tidal range also exhibits a process of variation from small to large and then to small. The duration of the rising tide is longer than that of the falling one, with an average difference of about 1 hour and 40 minutes. The duration difference of the neap tide is larger than that of the spring tide.

3.2. Tidal Current and Sediment Content. The sea area of the project is located on the arc-shaped coast of Shenquan Bay. Its upper promontory is from Aojiao to Yutou, and the lower promontory is the Jilan reef. There are two small flood discharge channels of Longjiang River and Leiling river system. The influence of geographical location, underwater topography, wave, and other factors adds complexity to the water flow in this area. The measured average velocity in the tidal section is 0.12 m/s, which can be recognized as a weak current area; The average velocity of rising and falling tides is 0.14 m/s and 0.10 m/s, respectively, and the velocity of the former is greater than that of the latter. Among the three water areas surveyed, the strongest flow intensity of all the three measuring stations is in the approach channel,

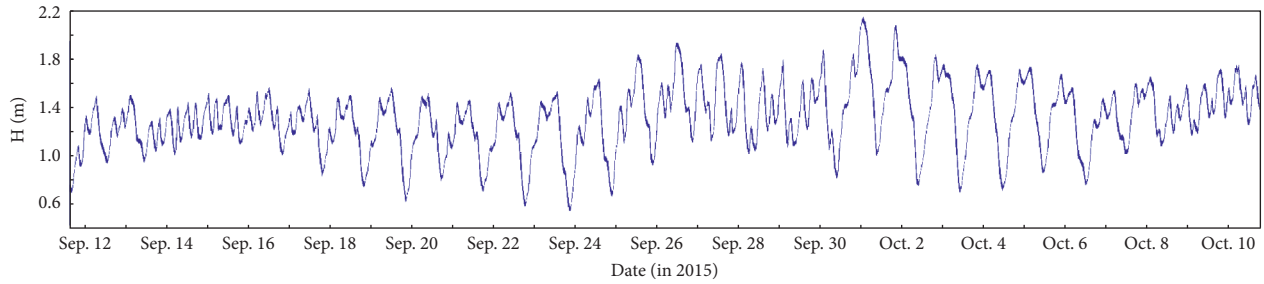

Figure 3: The tide level during Sep.12 to Oc. 10, 2015 in the study region.

followed by the Sinopec terminal and the proposed port area. The average velocities of rising and falling tides are 0.13 m/s, 0.12 m/s, and 0.09 m/s, respectively.

From Figures 4 and 5, it can be observed that in the project area, the average velocity of spring tide is less than that of the neap tide, being 0.09 m/s and 0.16 m/s, respectively, ascribing to strong winds and waves. In the proposed port area, the average velocities of rising and falling tides are 0.09 m/s and 0.10 m/s, respectively, and the average velocities of spring and neap tides are 0.07 m/s and 0.12 m/s, respectively. In the approach channel, the average velocity of rising tide is greater than that of the falling tide, being 0.18 m/s and 0.09 m/s, respectively, and the average velocities of spring and neap tides are 0.09 m/s and 0.17 m/s, respectively. In the water area of the Sinopec terminal, the average velocity of the rising tide is less than that of the falling tide, being 0.09 m/s and 0.15 m/s, respectively, ascribing to the breakwater on the east side, while the average velocities of spring and neap tides are 0.09 m/s and 0.15 m/s, respectively.

The sea area of the project is located in the arc-shaped coast of Shenquan Bay. Its upper promontory is from Aojiao to Yutou, and the lower promontory is the Jilan reef. There is no big river but two small flood discharge channels of Longjiang River and Leiling river system. The average annual water transmission of the former is $12 \times 10^8\ m^3$, and the annual suspended sediment discharge is 28×10^4 t, while the discharge of the latter is quite limited. During the observation, water in the sea is clear, which makes the water sample is basically clear with low sediment concentration.

The average sediment concentration of the spring tide and neap tide in the five measuring stations in this period is $0.010\ kg/m^3$, and the average sediment concentrations of rising and falling tides are $0.010\ kg/m^3$ and $0.011\ kg/m^{3,}$ respectively, which is basically the same. The maximum sediment concentrations of the instantaneous vertical line of rising and falling tides are $0.038\ kg/m^3$ and $0.040\ kg/m^{3,}$ respectively, which is observed in Station 4 in the Sinopec terminal. The average sediment concentration of spring tide is less than that of a neap tide, being $0.003\ kg/m^3$ and $0.018\ kg/m^{3,}$ respectively, ascribing to winds and waves. The average sediment concentrations of the proposed port, the approach channel, and the Sinopec terminal are $0.011\ kg/m^3$, $0.010\ kg/m^{3,}$ and $0.013\ kg/m^{3,}$ respectively, and the maximum sediment concentrations of the instantaneous vertical line are $0.026\ kg/m^3$, $0.032\ kg/m^3$, and $0.040\ kg/m^3$, respectively. The sediment concentration of the Sinopec terminal ranks first, followed by that of the proposed port and the approach channel, yet the difference is negligible. The hourly sediment concentration in each station fluctuates within a narrow range, independent of hourly velocity change (see Figure 5).

From the tidal current vector diagram (See Figure 6), it can be comprehended that the flow of rising and falling tides at each measuring station is basically rectilinear, except for that of Station 4. Compared with the tidal current, the residual current of the neap tide at stations 2 and 3 presents a high intensity, while that of other stations shows a low one, ranging from 0.02 to 0.10 m/s. The residual current generally moves in the direction of the rising tide (see Figure 7). Affected by the breakwater on the east side, the residual current in the neap tide period of station 4 moves in the direction of the falling tide.

The maximum vertical velocity of rising and falling tides at each measuring station is shown in Figure 8. The maximum vertical velocity of the rising tide is measured at station 2, being 0.59 m/s; that of the falling tide is measured at station 4, being 0.31 m/s. The velocities of rising and falling tides at station 2 are 0.57 m/s and 0.20 m/s, respectively, and the minimum velocities of rising and falling tides are measured at station 4, being 0.19 m/s and 0.17 m/s, respectively. There is a good correlation between the maximum vertical velocity of rising and falling tides and the average velocity of tidal sections, and the same results are obtained in this period (see Figure 8). Therefore, the distribution characteristics of the maximum vertical velocity of each water are validated by the average velocity of the discussed tidal sections.

3.3. Types of Sediment. The results of sample analysis are shown in Figure 9(a). The sediment in this area is coarse and fine. The median size ranges from 0.0041 mm to 0.2640 mm, with an average of 0.1037 mm, most of which are above 0.1000 mm. It can be seen from Figure 9(a) that the distribution of sediment presents a pattern of coarse near shore, fine in deep water, coarse in East and West, and fine in the middle.

The sorting coefficient of sediments in this area varies from 0.08 to 2.27. According to The Specification for Marine Monitoring [39], the sorting coefficient is divided into four grades, that is, 0–0.6 being well, 0.6–1.4 being medium well, 1.4–2.2 being medium, and >2.2 being poor. It can be seen from the table that more than half of the sediments are well,

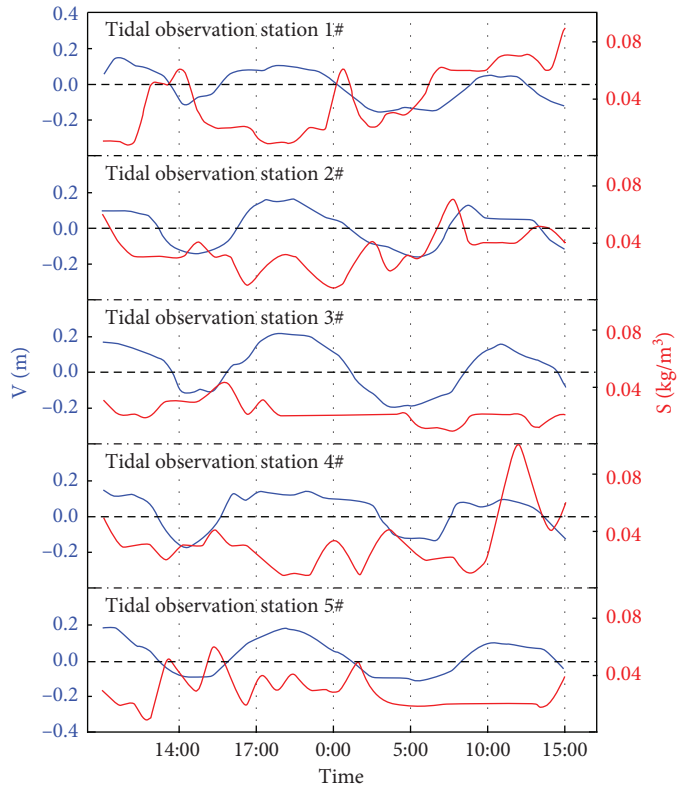

Figure 4: The vertical resultant velocity and sediment concentration of the spring tide during Sep. 22~23, 2015. The blue curves are the vertical resultant velocities at each tidal observation station corresponding to the left blue axis. The red curves are the sediment concentration measured at each tidal observation station corresponding to the right red axis.

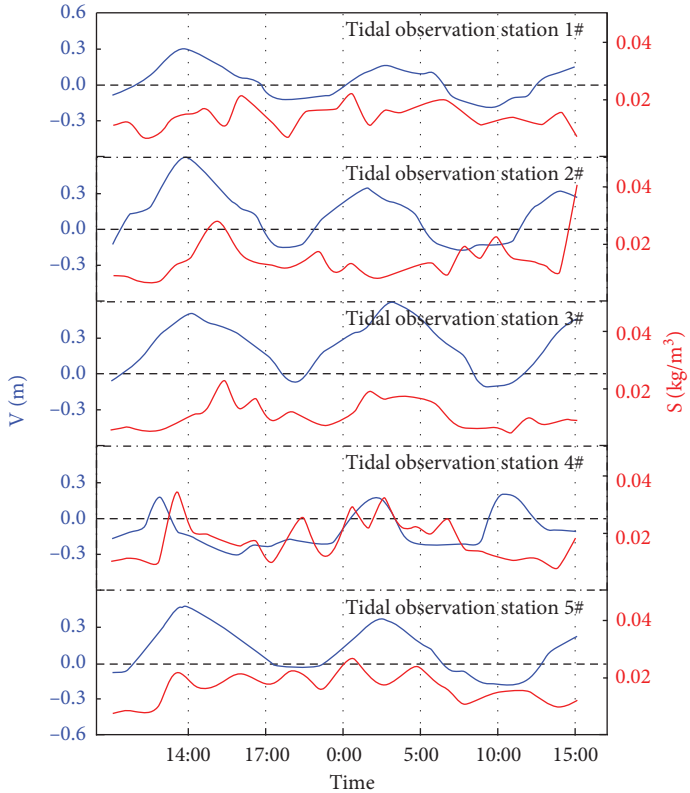

Figure 5: The vertical resultant velocity and sediment concentration of the neap tide during Sep. 22~23, 2015. The blue curves are the vertical resultant velocities at each tidal observation station corresponding to the left blue axis. The red curves are the sediment concentration measured at each tidal observation station corresponding to the right red axis.

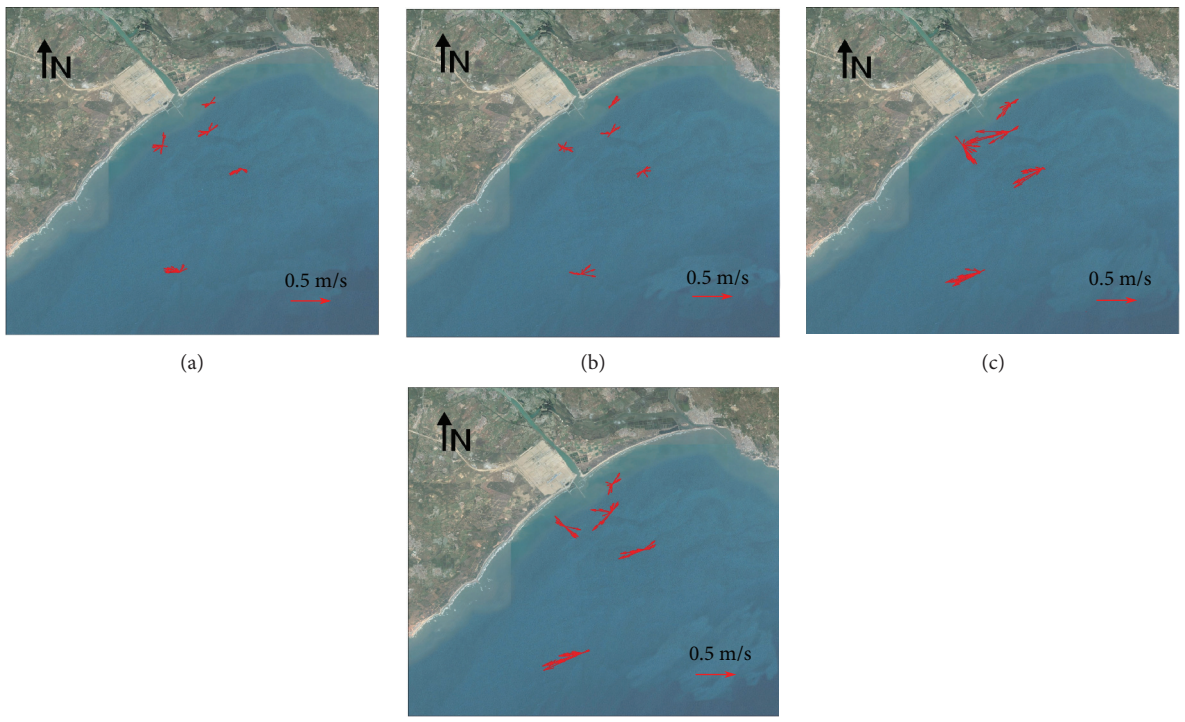

Figure 6: Tidal current vector diagram of tidal current and sediment observation in the study sea region, the velocity vectors indicate the depth average velocity. (a) The first tide cycle of the spring tide; (b) the second tide cycle of the spring tide; (c) the first cycle of the neap tide; (d) the second cycle of the neap tide.

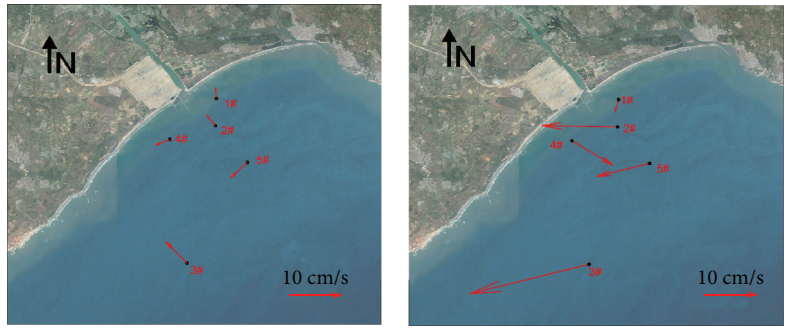

Figure 7: The residual current vector diagram of the study sea region, the velocity vectors indicate the depth average velocity. (a) The residual current of the spring tide; (b) the residual current of the neap tide.

accounting for 57.7%, followed by medium, accounting for 27.5%. It can be recognized from Figure 9(b) that in the nearshore shallow water area, the well (<0.6) are generally banded along the shore, indicating that the sediments are transported and sorted many times because of the waves. The medium well is in a long and narrow strip, and the poor exists only in a very small range. The sorting coefficient of other areas is between 1.4 and 2.2, being medium.

According to Figure 9(c), sediments with negative skewness are mainly located in the nearshore between the two estuaries, while the rest areas are with positive skewness. In the sampling area, sediments are mainly with positive skewness, and the grain size curve tends to the rough particle end. The wave control is dominant in this area, which presents a strong power of a wave in the nearshore. The results of the grain analysis are shown in Figure 9(d). It can be realized that there are five components in the sediment, namely, sands, coarse sand, medium coarse sand, fine sand, and silty clay. The fine sand is the majority, being 9.8%~98.1%, with an average of 66.1%, while the average content of clay is only 8.2%. The slope of the grain size distribution curve is steep.

Among the collected sediment samples, there are 8 types, which are coarse fine sand (CFS), medium fine sand (MFS), fine sand (FS), sand silt clay (STY), sandy silt (ST), clayey silt (YT), silt (T), and silty clay (TY). Among them, fine sand is

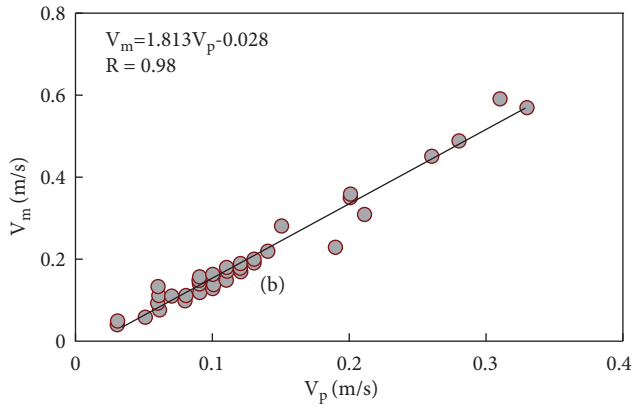

Figure 8: The correlation between the peak velocity and the average velocity.

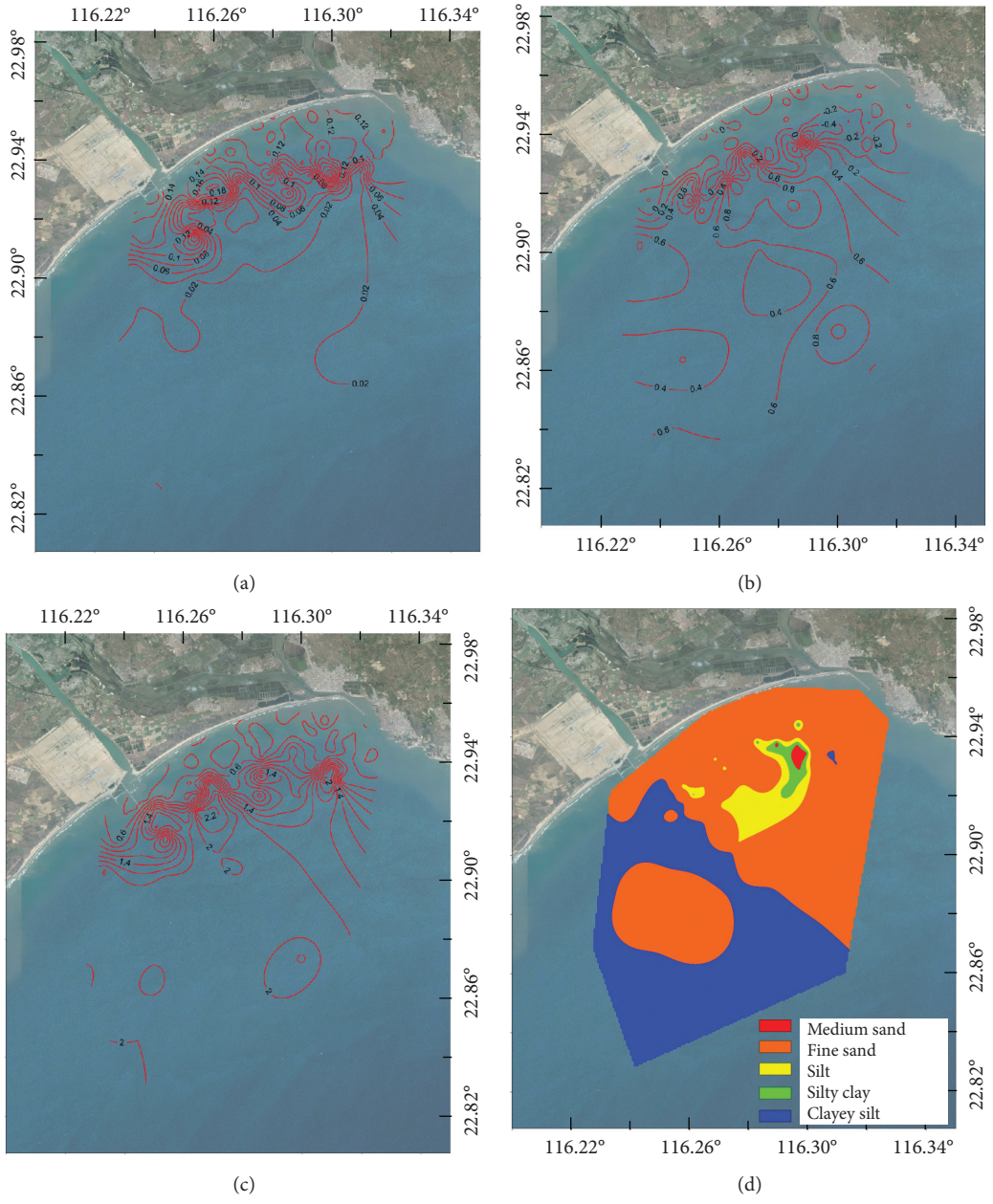

Figure 9: The distribution of the sediment in the study sea region. (a) The median particle size distribution of the sediment; (b) sorting degree distribution of the sediment; (c) the value of the skew distribution of the sediment; (d) the distribution of the classification of the sediment.

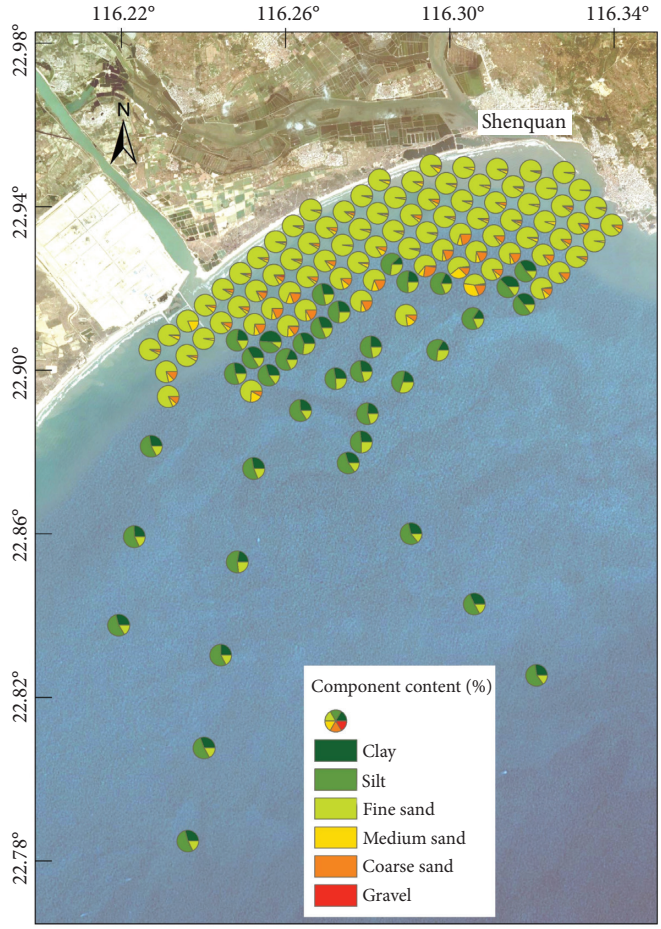

Figure 10: The sediment component content at the corresponding locations.

the majority, accounting for 66.4% (81) of the total sediment, while the rest is minor. According to the types of sediment, the study area can be divided into two parts, with the Longjiang estuary as the boundary, as shown in Figure 10. In the East, there are mainly fine sand, with a small amount of coarse fine sand, medium fine sand, sand silt clay, and other types. In the West, there is mainly clay silt, with a small amount of fine sand.

4. Conclusions

Coastal zone is a complex dynamic system, which is constantly affected by the change of sea level, sediment deposition, and erosion. Tide level, tidal current, suspended sediment, and surface sediment play a decisive role in the safe operation of the harbor. Therefore, based on the observation data of tide level, tidal current, suspended sediment, and surface sediment in the Port of Shenquan, this paper studied the characteristics of tidal current and sediment of projects in the sea area, and the following conclusions are drawn:

(1) The average tidal range during this period of observation is 0.6 m, which indicates that the Port of Shenquan is with weak tides. From the measured tide hydrograph, it can be comprehended that the tide in the Port of Shenquan is irregular diurnal. Ascribing to the influence of geographical location and shallow water constituent, the tidal curve presents an obvious deformation, with a small fluctuation in the high tide period and frequent fluctuations in the spring tide process of the neap tide.

(2) The tide in the study area is semidiurnal, and the flow of rising and falling tides is rectilinear. The average velocity of tide section measured is 0.12 m/s, which indicates that it is with weak tides. The approach channel ranks first in water flow intensity, followed by the Sinopec terminal and the proposed port. The velocity of flow of the neap tide is larger than that of spring tide, ascribing to strong winds and waves.

(3) The study area is with no large river into the sea and a limited source of sand. During the observation, water in the sea is clear, which makes the water sample basically clear with low sediment concentration. The average sediment concentration measured in this period is 0.010 kg/m3, which is basically the same. The maximum sediment concentrations of the instantaneous vertical line of rising and falling tides are 0.038 kg/m3 and 0.040 kg/m3, respectively. The

Sinopec terminal ranks first in sediment, followed by the proposed port area and the approach channel. The hourly sediment concentration in each station fluctuates within a narrow range, independent of hourly velocity change.

(4) The sediment in the study area is coarse and fine, with an average grain size of 0.1037 mm. The distribution of it presents a pattern of coarse near shore, fine in deep water, coarse in East and West, and fine in the middle. The sorting coefficient is medium to well and the majority of the sediment is fine sand, accounting for 66.1%, while the amount of the clay is 8.2%. According to the types of sediment, the study area can be divided into two parts, with the Longjiang estuary as the boundary. In the East, there is mainly fine sand, with a small amount of coarse fine sand, medium fine sand, sand silt clay, and other types. In the West, there is mainly clay silt, with a small amount of fine sand.

Data Availability

All data related to this paper are available from the authors upon request.

Conflicts of Interest

The authors declare no conflicts of interest.

Acknowledgments

This research was funded by the National Natural Science Foundation of China, grant no. U2040203.

References

[1] T. A. Labuz, "Environmental impacts-coastal erosion and coastline changes," *Second Assessment of Climate Change for the Baltic Sea Basin*, pp. 381–396, Springer, Berlin, Germany, 2015.

[2] K. Yokoyama and K. W. Suzuki, "Sediment transport, morphodynamics and estuarine production in the Chikugo River," *Nippon Suisan Gakkaishi*, vol. 83, no. 6, Article ID 1015, 2017.

[3] A. Hibma, M. J. F. Stive, and Z. B. Wang, "Estuarine morphodynamics," *Coastal Engineering*, vol. 51, no. 8-9, pp. 765–778, 2004.

[4] H. Tanaka and H. Chanson, "Estuarine hydrodynamics and morphodynamics: a perspective," *Coastal Engineering Journal*, vol. 60, no. 4, pp. 385-386, 2018.

[5] W. Wei, Z. J. Dai, X. F. Mei, J. P. Liu, S. Gao, and S. Li, "Shoal morphodynamics of the Changjiang (Yangtze) estuary: influences from river damming, estuarine hydraulic engineering and reclamation projects," *Marine Geology*, vol. 386, pp. 32–43, 2017.

[6] P. Gurumurthy, P. M. Orton, S. A. Talke, S. A. Georgas, and J. F. Booth, "Mechanics and historical evolution of sea level blowouts in New York harbor," *Journal of Marine Science and Engineering*, vol. 7, no. 5, p. 160, 2019.

[7] S. C. Yan, S. F. Lin, and G. P. Chen, "Three-dimensional wave basin model test for general-purpose wharf in Jinghai district of Jieyang Harbor," *Advances in Civil and Industrial Engineering*, vol. 353-356, pp. 2724–2731, 2013.

[8] H. L. Zhong, Y. S. Lin, T. L. Yip, W. Cai, and Y. Gu, "A novel oil port risk and efficiency performance measured by using AIS data and maritime open data: the case of Guangzhou, China," *Ocean Engineering*, vol. 216, Article ID 107859, 2020.

[9] W. Tang, W. Zhan, B. W. Jin, M. Motagh, and Y. Xu, "Spatial variability of relative sea-level rise in Tianjin, China: insight from InSAR, GPS, and tide-gauge observations," *IEEE Journal of Selected Topics in Applied Earth Observations and Remote Sensing*, vol. 14, pp. 2621–2633, 2021.

[10] A. Ilia and J. O'Donnell, "An assessment of two models of wave propagation in an estuary protected by breakwaters," *Journal of Marine Science and Engineering*, vol. 6, no. 4, 2018.

[11] H. Zheng, D. Wang, and R. P. Behringer, "Experimental study on granular biaxial test based on photoelastic technique," *Engineering Geology*, vol. 260, Article ID 105208, 2019.

[12] Z. Dou, S. Tang, X. Zhang et al., "Influence of shear displacement on fluid flow and solute transport in a 3D rough fracture," *Lithosphere*, vol. 2021, Article ID 1569736, 2021.

[13] Z. Dou, Y. Liu, X. Zhang et al., "Influence of layer transition zone on rainfall-induced instability of multilayered slope," *Lithosphere*, vol. 2021, Article ID 2277284, 2021.

[14] B. Ramakrishnan, N. P. Singh, and S. Jeyaraj, "Input reduction and acceleration techniques in a morphodynamic modeling: a case study of Mumbai harbor," *Regional Studies in Marine Science*, vol. 31, Article ID 100765, 2019.

[15] T. P. Austin, A. D. Short, M. G. Hughes, A. Vila-Concejo, and R. Ranasinghe, "Tidal hydrodynamics of a micro-tidal, wave dominated flood-tide delta: Port Stephens, Australia," *Journal of Coastal Research*, vol. SI, pp. 693–697, 2009.

[16] R. W. Brander, P. S. Kench, and D. Hart, "Spatial and temporal variations in wave characteristics across a reef platform, Warraber Island, Torres Strait, Australia," *Marine Geology*, vol. 207, no. 1–4, pp. 169–184, 2004.

[17] J. C. Warner, C. R. Sherwood, R. P. Signell, C. Harris, and H. G. Arango, "Development of a three-dimensional, regional, coupled wave, current, and sediment-transport model," *Computers & Geosciences*, vol. 34, no. 10, pp. 1284–1306, 2008.

[18] L. Han, L. Wang, X. Ding, H. Wen, X. Yuan, and W. Zhang, "Similarity quantification of soil parametric data and sites using confidence ellipses," *Geoscience Frontiers*, vol. 13, no. 1, Article ID 101280, 2022.

[19] D. Wang, H. Zheng, Y. Ji, J. Bares, and R. P. Behringer, "Shear of granular materials composed of ellipses," *Granular Matter*, vol. 22, no. 1, 2020.

[20] A. M. Bernabeu, A. V. Lersundi-Kanpistegi, and F. Vilas, "Gradation from oceanic to estuarine beaches in a ria environment: a case study in the Ria de Vigo," *Estuarine, Coastal and Shelf Science*, vol. 102, pp. 60–69, 2012.

[21] N. L. Jackson, K. F. Nordstrom, I. Eliot, and G. Masselink, ""Low energy" sandy beaches in marine and estuarine environments: a review," *Geomorphology*, vol. 48, no. 1–3, pp. 147–162, 2002.

[22] M. D. Harley, I. L. Turner, and A. D. Short, "New insights into embayed beach rotation: the importance of wave exposure and cross-shore processes," *Journal of Geophysical Research-Earth Surface*, vol. 120, no. 8, pp. 1470–1484, 2015.

[23] R. Kian, D. Velioglu, A. C. Yalciner, and A. Zaytsev, "Effects of harbor shape on the induced sedimentation; L-type basin," *Journal of Marine Science and Engineering*, vol. 4, no. 3, Article ID 55, 2016.

[24] Y. S. Wu, J. Chaffey, D. A. Greenberg, K. Colbo, and P. C. Smith, "Tidally-induced sediment transport patterns in

the upper Bay of Fundy: a numerical study," *Continental Shelf Research*, vol. 31, no. 19, pp. 2041–2053, 2011.

[25] L. Q. Zuo, D. Roelvink, and Y. J. Lu, "The mean suspended sediment concentration profile of silty sediments under wave-dominant conditions," *Continental Shelf Research*, vol. 186, pp. 111–126, 2019.

[26] Z. H. Wu, B. Yang, and Y. He, "Experimental study on suspended sediment concentration and powder bed deformation under wave-only and wave-with-current scenarios," in *Proceedings of the 5th International Conference on Coastal and Ocean Engineering (ICCOE 2018)*, Shanghai, China, April 2018.

[27] H. Zheng, D. Wang, X. M. Tong, L. Li, and R. P. Behringer, "Granular scale responses in the shear band region," *Granular Matter*, vol. 21, no. 4, 2019.

[28] Y. Q. Zhao, J. Bares, H. Zheng, J. E. S. Socolar, and R. P. Behringer, "Shear-jammed, fragile, and steady states in homogeneously strained granular materials," *Physical Review Letters*, vol. 123, no. 15, Article ID 158001, 2019.

[29] B. Yuan, M. Sun, Y. Wang, and L. Zhai, "Full 3D displacement measuring system for 3D displacement field of soil around a laterally loaded pile in transparent soil," *International Journal of Geomechanics*, vol. 19, no. 5, 2019.

[30] Y. S. Wu, C. G. Hannah, M. O'Flaherty-Sproul, P. MacAulay, and S. Shan, "A modeling study on tides in the Port of Vancouver," *Anthropocene Coasts*, vol. 2, no. 1, pp. 101–125, 2019.

[31] H. Karunarathna, D. Reeve, and M. Spivack, "Long-term morphodynamic evolution of estuaries: an inverse problem," *Estuarine, Coastal and Shelf Science*, vol. 77, no. 3, pp. 385–395, 2008.

[32] S. P. Neill, E. J. Litt, S. J. Couch, and A. G. Davies, "The impact of tidal stream turbines on large-scale sediment dynamics," *Renewable Energy*, vol. 34, no. 12, pp. 2803–2812, 2009.

[33] R. Sanay, G. Voulgaris, and J. C. Warner, "Tidal asymmetry and residual circulation over linear sandbanks and their implication on sediment transport: a process-oriented numerical study," *Journal of Geophysical Research-Oceans*, vol. 112, no. 12, 2007.

[34] J. R. Lacy, M. C. Ferner, and J. C. Callaway, "The influence of neap-spring tidal variation and wave energy on sediment flux in salt marsh tidal creeks," *Earth Surface Processes and Landforms*, vol. 43, no. 11, pp. 2384–2396, 2018.

[35] C. Q. Zhu, X. L. Liu, H. X. Shan et al., "Properties of suspended sediment concentrations in the Yellow River delta based on observation," *Marine Georesources & Geotechnology*, vol. 36, no. 1, pp. 139–149, 2018.

[36] G. X. Li, L. L. Qiao, P. Dong et al., "Hydrodynamic condition and suspended sediment diffusion in the yellow sea and east China sea," *Journal of Geophysical Research-Oceans*, vol. 121, no. 8, pp. 6204–6222, 2016.

[37] C. Venier, A. D'Alpaos, and M. Marani, "Evaluation of sediment properties using wind and turbidity observations in the shallow tidal areas of the Venice Lagoon," *Journal of Geophysical Research-Earth Surface*, vol. 119, no. 7, pp. 1604–1616, 2014.

[38] B. Yuan, Z. Li, Y. Chen et al., "Mechanical and microstructural properties of recycling granite residual soil reinforced with glass fiber and liquid-modified polyvinyl alcohol polymer," *Chemosphere*, vol. 286, 2022.

[39] National Standards of the People's Republic of China, *The Specification for Marine Monitoring (GB/T 14914.1-2018)*, China Communications Press, Beijing, China, 2018, in Chinese.